NASA Technical Memorandum 4644

Shear Buckling Analysis of a Hat-Stiffened Panel

William L. Ko and Raymond H. Jackson

November 1994

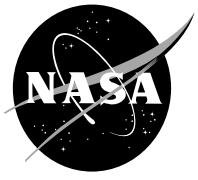

NASA Technical Memorandum 4644

Shear Buckling Analysis of a Hat-Stiffened Panel

William L. Ko and Raymond H. Jackson
Dryden Flight Research Center
Edwards, California

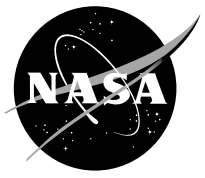

National Aeronautics and
Space Administration

Office of Management

Scientific and Technical
Information Program

1994

ABSTRACT

A buckling analysis was performed on a hat-stiffened panel subjected to shear loading. Both local buckling and global buckling were analyzed. The global shear buckling load was found to be several times higher than the local shear buckling load. The classical shear buckling theory for a flat plate was found to be useful in predicting the local shear buckling load of the hat-stiffened panel, and the predicted local shear buckling loads thus obtained compare favorably with the results of finite element analysis.

NOMENCLATURE

A	cross-sectional area of one corrugation leg, $A = lt_c$, in^2
$\bar{A}$	cross-sectional area of global panel segment bounded by p, $\bar{A} = A + pt_s + \frac{1}{2}(f_1 - f_2)t_c$, in^2
A_{mn}	Fourier coefficient of assumed trial function for $w(x, y)$, in.
a	length of global panel, in.
b	horizontal distance between centers of corrugation and curved region, $b = \frac{1}{2}\left[p - \frac{1}{2}(f_1 + f_2)\right]$, in.
b_o	width of rectangular flat plate segment, in.
c	width of global panel, in.
D	flexural rigidity of flat plate, $D = \frac{E_s t_s^3}{12(1 - \nu_s^2)}$, in-lb
D^*	flexural stiffness parameter, $\sqrt{\bar{D}_x \bar{D}_y}$, in-lb
D_{Qx}, D_{Qy}	transverse shear stiffnesses in xz-, yz-planes, lb/in
D_x, D_y, D_{xy}	effective bending stiffnesses of equivalent hat-stiffened panel, in-lb
d	one-half of diagonal region of corrugation leg, in.
E_c	modulus of elasticity of hat material, lb/in^2
E_s	modulus of elasticity of face sheet material, lb/in^2
f_1	lower flat region of hat stiffener, in.
f_2	upper flat region of hat stiffener, in.
G_c	shear modulus of hat material, lb/in^2
G_s	shear modulus of face sheet material, lb/in^2
h	distance between middle surfaces of hat top flat region and face sheet, $h = h_c + \frac{1}{2}(t_c + t_s)$, in.
h_c	distance between middle surfaces of hat upper and lower flat regions, in.

h_o	distance between middle surface of face sheet and centroid of global panel segment, in.
I_c	moment of inertia, per unit width, of corrugation leg, $\frac{1}{12}t_c^3$, in^4/in
$\overline{I}_c$	moment of inertia, per unit width, of one-half of reinforcing hat taken with respect to the neutral axis η_o of the hat stiffened panel, in^4/in
I_c^*	moment of inertia of corrugation leg of length *l* taken with respect to its neutral axis η, in^4
I_f	moment of inertia, per unit width, of corrugation flat region $\frac{1}{12}t_c^3$, in^4/in
I_s	moment of inertia, per unit width, of face sheet with respect to η_o axis passing through the centroid of the global panel segment, $I_s = t_s h_o^2 + \frac{1}{12}t_s^3$, in^4/in
I_s'	moment of inertia, per unit width, of face sheet and corrugation flat region combined, $\frac{1}{12}(t_s + t_c)^3$, in^4/in
k_{xy}	shear buckling load factor
l	length of corrugation leg, $l = f_2 + 2d + 2R\theta$, in.
$\overline{l}$	length of one-half of hat, $\overline{l} = l + \frac{1}{2}(f_1 - f_2)$, in.
m	number of buckle half-waves in x-direction
N_{xy}	panel shear load, lb/in
n	number of buckle half-waves in y-direction
p	one half of reinforcing hat pitch, in.
Q_{cr}	shear buckling load, lb
q_1	shear flow in flat panel, lb/in
q_c	shear flow in hat, lb/in
R	radius of circular arc segments of corrugation leg, in.
t_c	thickness of reinforcing hat, in.
t_s	thickness of face sheet, in.
w	panel out-of-plane displacement, in.
x, y	rectangular Cartesian coordinates, in.
$\frac{\partial^2 w}{\partial x \partial y}$	panel twist, 1/in
η_o	neutral axis of corrugation leg and face sheet combined

θ	corrugation angle (angle between the face sheet and the straight diagonal segment of corrugation leg), rad
ν_c	Poisson ratio of hat material
ν_s	Poisson ratio of face sheet material
τ_{xy}	shear stress, lb/in^2
$(\ )_{cr}$	critical value at buckling

INTRODUCTION

Recently, various hot-structural panel concepts were advanced for applications to hypersonic aircraft structural panels. Among those panels investigated, the hat-stiffened panel (fig. 1) was found to be an excellent candidate for potential application to hypersonic aircraft fuselage panels. This type of panel is equivalent to a corrugated core sandwich panel with one face sheet removed.

Buckling behavior of the hat-stiffened panel under compressive loading in the hat-axial direction, was investigated by Ko and Jackson recently (ref. 1). They calculated both the local and global (general panel instability) compressive buckling loads for the panel. The calculated local compressive buckling load was found to be far lower than the global compressive buckling load, and compared fairly well with the experimental data. To fully understand buckling characteristics of the hat-stiffened panel, the shear buckling behavior of this panel needs to be investigated.

This report presents the local and global buckling analyses of the hat-stiffened panel subjected to shear loading. The predicted shear buckling loads are compared with the finite element shear buckling solutions.

SHEAR BUCKLING ANALYSIS

To analyze the buckling behavior of the complex structure shown in figure 1, two approaches were taken: (1) local buckling analysis, and (2) global buckling analysis (general panel instability). The following sections describe these approaches.

Local Buckling

The purpose of local buckling analysis was to study the buckling behavior of a local weak region of the panel. This weak region is identified as a rectangular flat plate region bounded by two legs of the reinforcing hat located at the center of the global panel (left diagram of fig. 2). The analysis looked at the buckling behavior of this rectangular flat plate (slender strip). Because the reinforcing hat has high flexural rigidity, the four edges of the rectangular plate were assumed to be simply supported (right diagram of fig. 2). From reference 2, the shear buckling stress $(\tau_{xy})_{cr}$ in the rectangular flat plate may be written as

$$(\tau_{xy})_{cr} = k_{xy} \frac{\pi^2 D}{b_o^2 t_s} \tag{1}$$

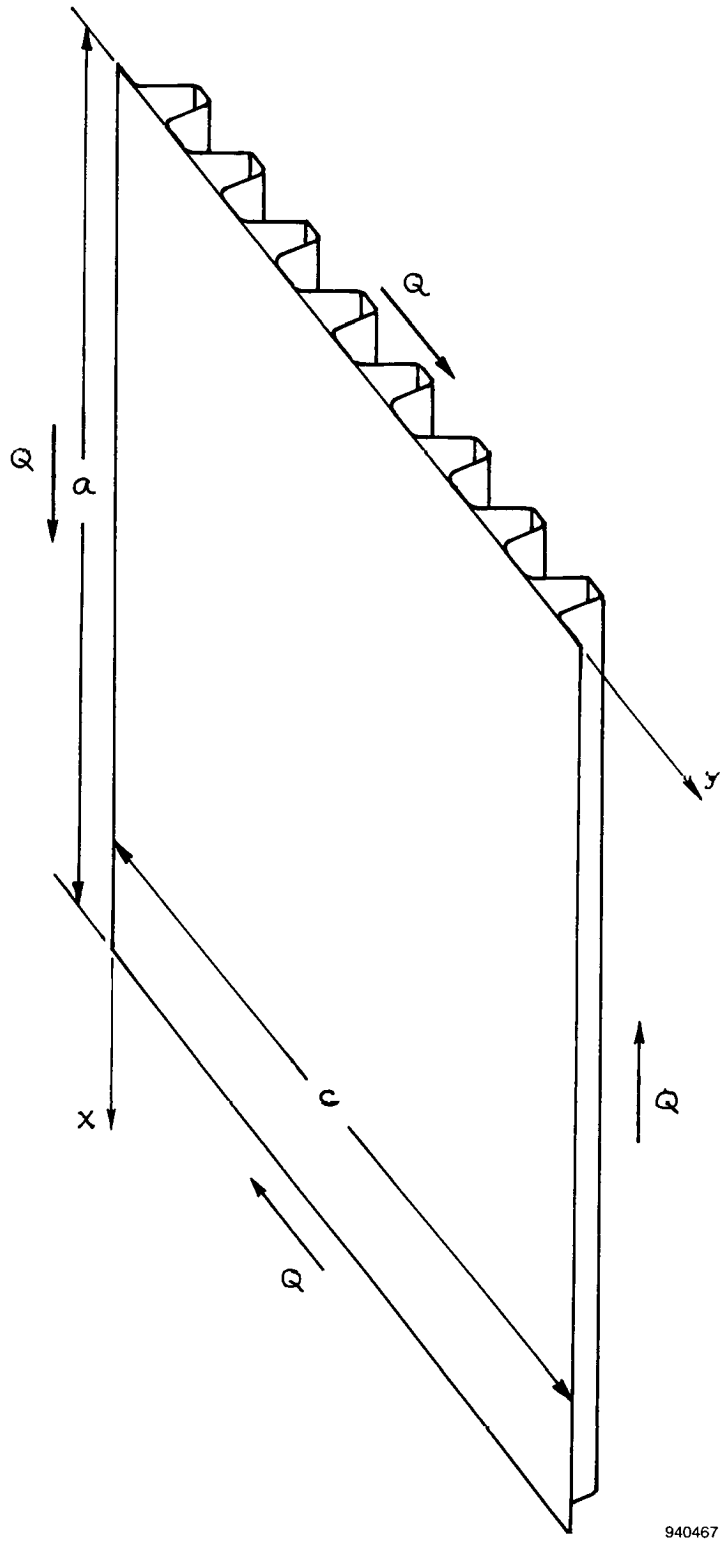

Figure 1. Hat-stiffened panel under shear loading.

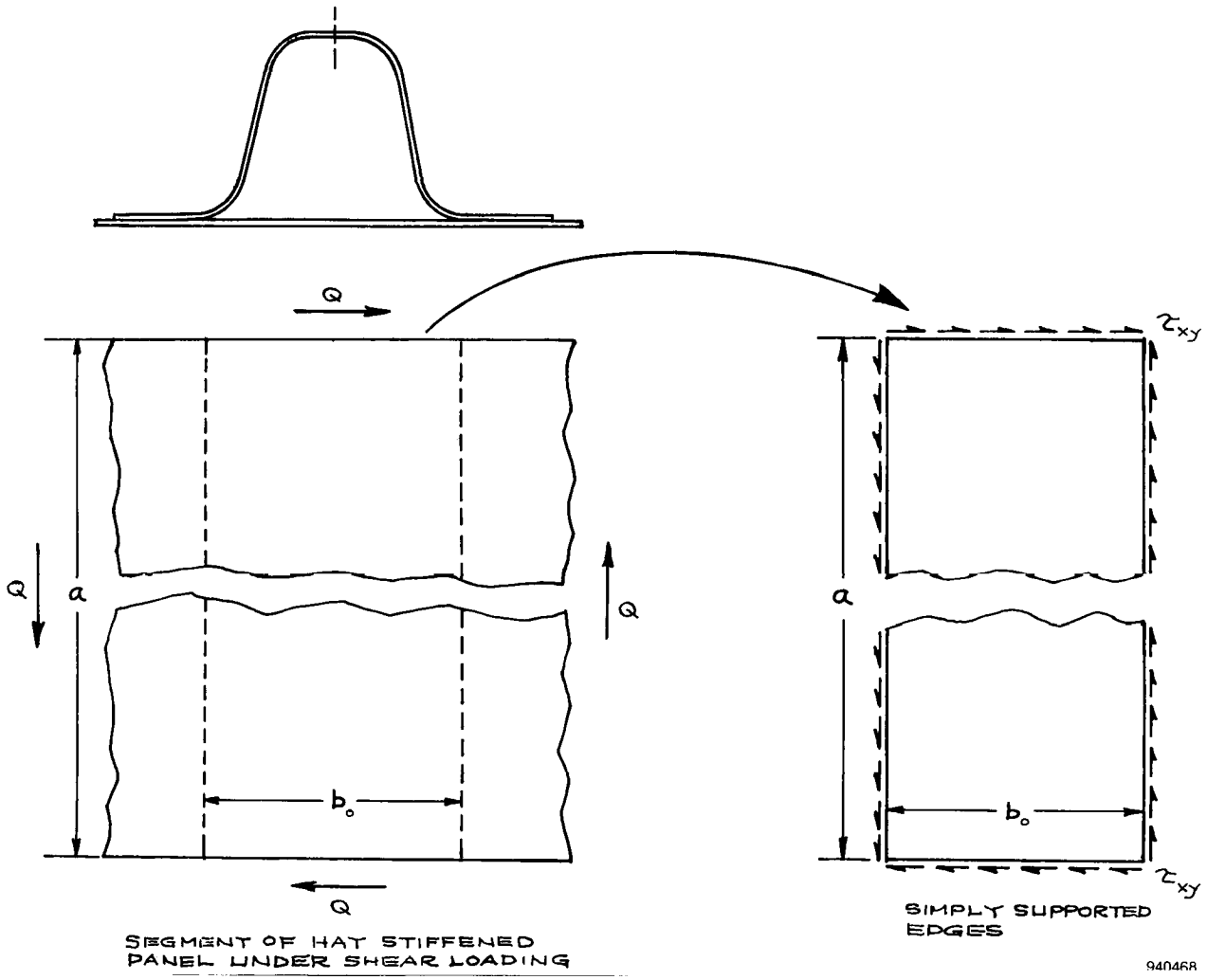

Figure 2. Shear buckling of hat-stiffened panel analyzed using a simple model.

where k_{xy} is the shear buckling load factor, which is a function of panel aspect ratio $\frac{b_o}{a}$. For $\frac{b_o}{a} = 1$ (a square panel), $k_{xy} = 9.34$; and for $\frac{b_o}{a} = 0$ (an infinitely long panel), $k_{xy} = 5.35$. For intermediate values of $\frac{b_o}{a}$, k_{xy} may be found from a parabolic curve-fitting equation of the form (ref. 2)

$$k_{xy} = 5.35 + 4\left(\frac{b_o}{a}\right)^2 \tag{2}$$

The curve described by equation (2) is shown on the left in figure 3. The panel shear load N_{xy} for the hat-stiffened strip (left diagram of fig. 2) may be written in terms of shear flows (fig. 4) as (ref. 4)

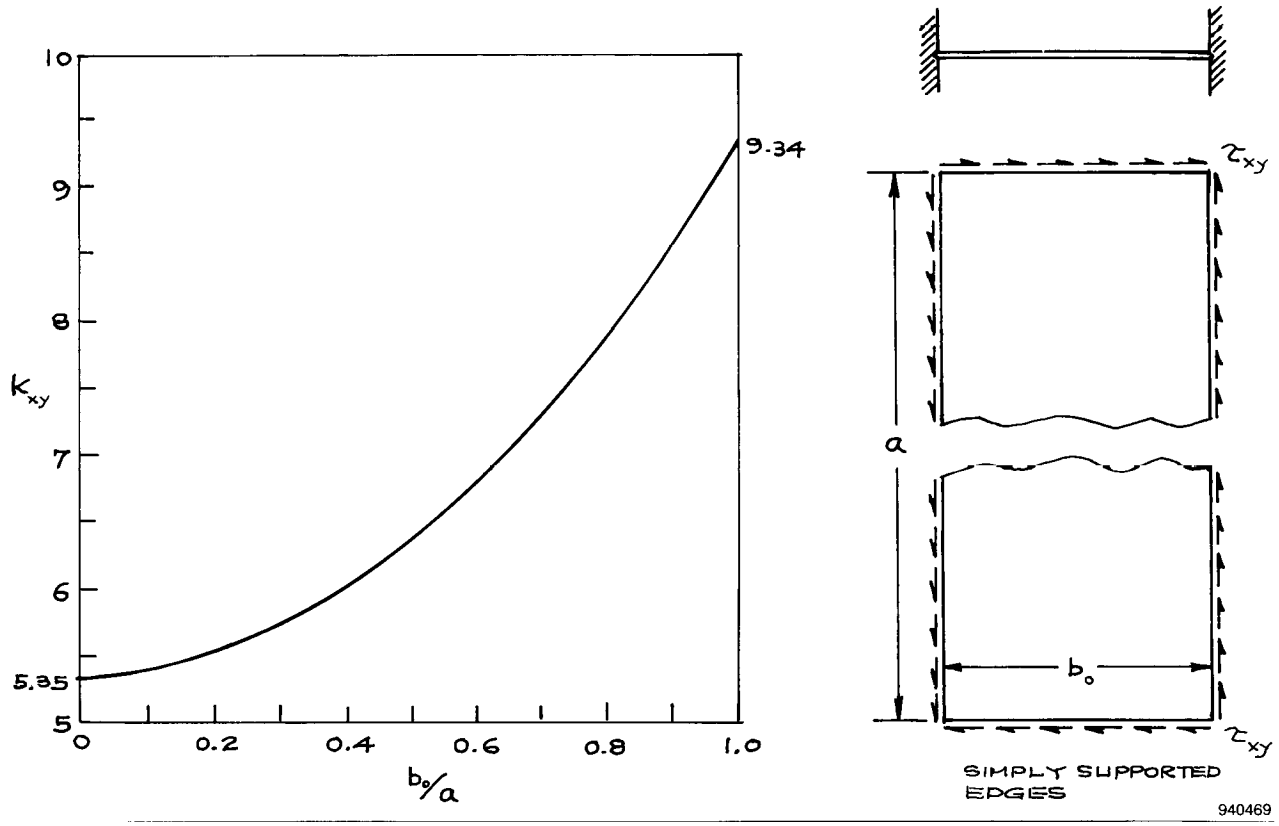

Figure 3. Shear buckling load parameter as a function of panel aspect ratio.

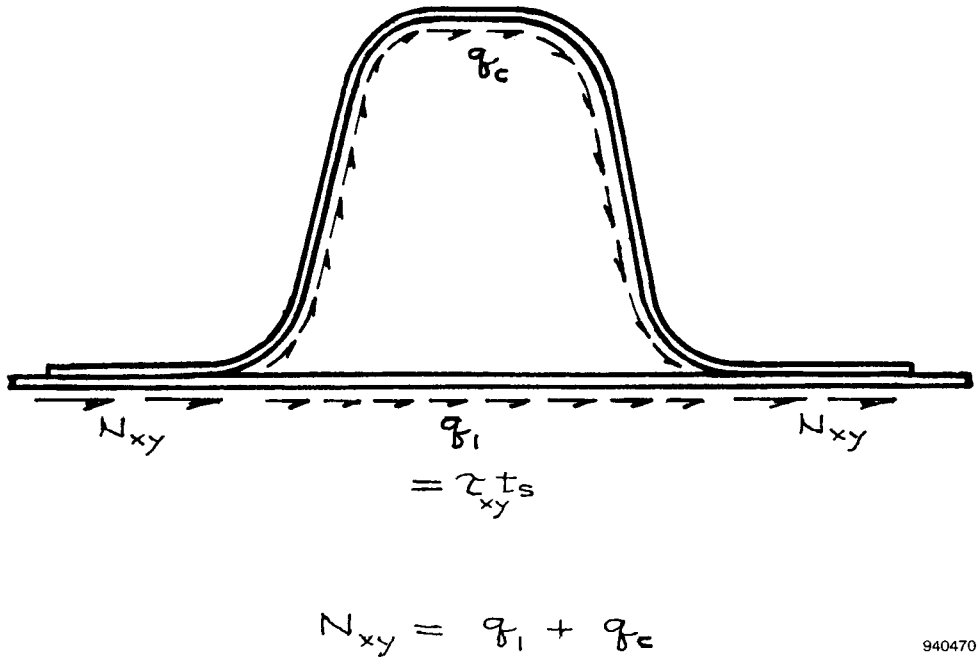

Figure 4. Shear flows in the reinforcing hat and the flat region under the hat.

$$N_{xy} = q_1 + q_c \tag{3}$$

where q_1 and q_c are, respectively, the shear flows in the flat panel and the hat, and are given by (ref. 4)

$$q_1 = \tau_{xy} t_s = 2G_s h_o t_s \frac{\partial^2 w}{\partial x \partial y} \tag{4}$$

and

$$q_c = \frac{G_c t_c p}{l}\left[h - 2h_o - \frac{h_c}{2p}(f_1 - f_2)\right]\frac{\partial^2 w}{\partial x \partial y} \tag{5}$$

where $\frac{\partial^2 w}{\partial x \partial y}$ is the panel twist.

From equations (4) and (5), the ratio q_1/q_c may be calculated. Then, from equation (3), the panel shear buckling load $(N_{xy})_{cr}$ of the hat-stiffened strip may be calculated as a function of $(\tau_{xy})_{cr}$ (eq. (1)).

Global Buckling

In the global buckling analysis (general instability analysis), the complex panel was represented by a homogeneous anisotropic panel having effective elastic constants. These effective elastic constants must be calculated first (ref. 3). This analysis is similar to the conventional buckling analysis of a sandwich panel with one face sheet removed.

By using the small-deflection theory developed for flat sandwich plates (ref. 5) and solving the shear buckling problem of the hat-stiffened plate using the Rayleigh-Ritz method of minimizing the total potential energy of a structural system (refs. 5 through 9), the following shear buckling equation is obtained:

$$\frac{M_{mn}}{k_{xy}} A_{mn} + \sum_{i=1}^{\infty}\sum_{j=1}^{\infty} \delta_{mnij} A_{ij} = 0 \tag{6}$$

where

$$M_{mn} = \frac{1}{32}\frac{ab}{D^*}\left(\frac{a}{\pi}\right)^2\left[a_{mn}^{11} + \underbrace{\frac{a_{mn}^{12}(a_{mn}^{23}a_{mn}^{31} - a_{mn}^{21}a_{mn}^{33}) + a_{mn}^{13}(a_{mn}^{21}a_{mn}^{32} - a_{mn}^{22}a_{mn}^{31})}{a_{mn}^{22}a_{mn}^{33} - a_{mn}^{23}a_{mn}^{32}}}\right] \tag{7}$$

classical thin plate theory — transverse shear effect terms

$$\delta_{mnij} \equiv \frac{mnij}{(m^2 - i^2)(n^2 - j^2)}; \quad \begin{matrix} m \neq i, n \neq j, \\ m \pm i = \text{odd}, \; n \pm j = \text{odd} \end{matrix} \tag{8}$$

and A_{mn} are the undetermined Fourier coefficients of the assumed out-of-plane displacement w (x, y) of the plate given by

$$w(x, y) = \sum_{m=1}^{\infty} \sum_{n=1}^{\infty} A_{mn} \sin \frac{m\pi x}{a} \sin \frac{n\pi y}{c} \tag{9}$$

Lastly, the shear buckling load factor k_{xy} appearing in equation (6) and the coefficients of characteristic equation $a_{mn}^{rs}(r, s = 1, 2, 3)$ appearing in equation (7) are defined, respectively, as (ref. 7)

$$k_{xy} = \frac{(N_{xy})_{cr} a^2}{\pi^2 D^*} \tag{10}$$

$$a_{mn}^{11} = \bar{D}_x \left(\frac{m\pi}{a}\right)^4 + (\bar{D}_x \nu_{yx} + \bar{D}_y \nu_{xy} + 2D_{xy}) \left(\frac{m\pi}{a}\right)^2 \left(\frac{n\pi}{c}\right)^2 + \bar{D}_y \left(\frac{n\pi}{c}\right)^4 \tag{11}$$

$$a_{mn}^{12} = a_{mn}^{21} = -\left[\bar{D}_x \left(\frac{m\pi}{a}\right)^3 + \frac{1}{2} (\bar{D}_x \nu_{yx} + \bar{D}_y \nu_{xy} + 2D_{xy}) \left(\frac{m\pi}{a}\right) \left(\frac{n\pi}{c}\right)^2\right] \tag{12}$$

$$a_{mn}^{13} = a_{mn}^{31} = -\left[\bar{D}_y \left(\frac{n\pi}{c}\right)^3 + \frac{1}{2} (\bar{D}_x \nu_{yx} + \bar{D}_y \nu_{xy} + 2D_{xy}) \left(\frac{m\pi}{a}\right)^2 \left(\frac{n\pi}{c}\right)\right] \tag{13}$$

$$a_{mn}^{22} = \bar{D}_x \left(\frac{m\pi}{a}\right)^2 + \frac{D_{xy}}{2} \left(\frac{n\pi}{c}\right)^2 + D_{Qx} \tag{14}$$

$$a_{mn}^{23} = a_{mn}^{32} = \frac{1}{2} (\bar{D}_x \nu_{yx} + \bar{D}_y \nu_{xy} + D_{xy}) \left(\frac{m\pi}{a}\right) \left(\frac{n\pi}{c}\right) \tag{15}$$

$$a_{mn}^{33} = \bar{D}_y \left(\frac{n\pi}{c}\right)^2 + \frac{D_{xy}}{2} \left(\frac{m\pi}{a}\right)^2 + D_{Qy} \tag{16}$$

where the flexural stiffness parameter D^* and the flexural rigidities of the effective panel $\bar{D}_x, \bar{D}_y$ are defined as

$$D^* = \sqrt{\bar{D}_x \bar{D}_y}, \quad \bar{D}_x = \frac{D_x}{1 - \nu_s^2}, \quad \bar{D}_y = \frac{D_y}{1 - \nu_s^2} \tag{17}$$

where

$$D_x = E_c \bar{I}_c + E_s I_s, \quad D_y = E_s I_s \frac{1 + \dfrac{E_c \bar{I}_c}{E_s I_s}}{1 + (1 - \nu_s^2) \dfrac{E_c \bar{I}_c}{E_s I_s}} \tag{18}$$

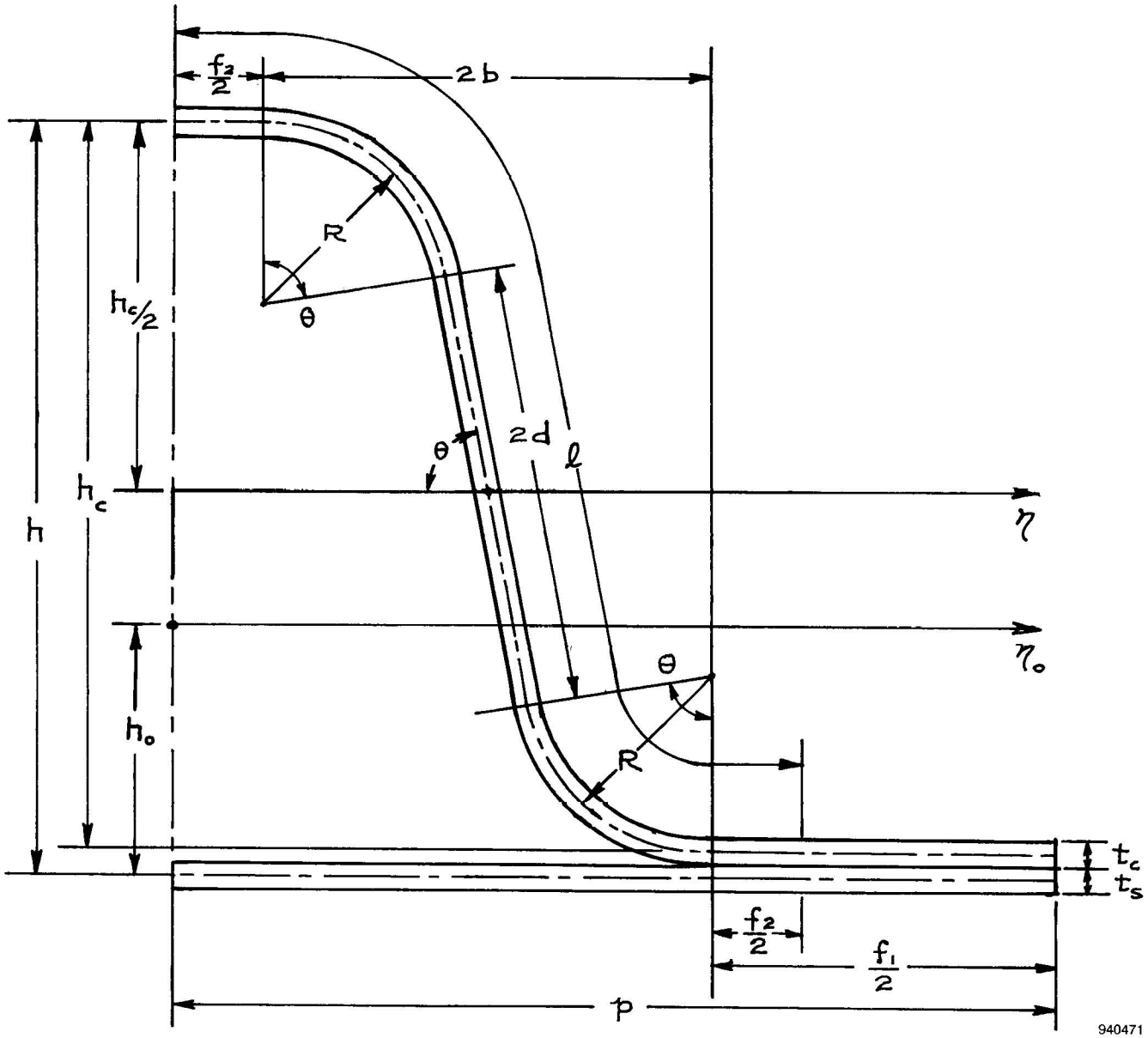

Figure 5. Segment of hat-stiffened flat panel.

where

$$I_s = t_s h_o^2 + \frac{1}{12} t_s^3 \tag{19}$$

and $\bar{I}_c$ is the moment of inertia, per unit width, taken with respect to the panel neutral axis η_o (fig. 5), and is given by

$$\bar{I}_c = \frac{I_c^*}{p} + \frac{A}{p}\left[\frac{1}{2}(h_c + t_c + t_s) - h_o\right]^2 + \frac{1}{24p}(f_1 - f_2)t_c^3 + \frac{f_1 - f_2}{2p} t_c \left(h_o - \frac{t_c + t_s}{2}\right)^2 \tag{20}$$

where I_c^* is the moment of inertia of a corrugation leg of length *l*, taken with respect to its neutral axis η (fig. 5), and is given by

$$I_c^* = h_c^3 t_c \left\{ \frac{1}{4}\frac{f_2}{h_c}\left(1 + \frac{1}{3}\frac{t_c^2}{h_c^2}\right) + \frac{2}{3}\frac{d^3}{h_c^3}\left(\sin^2\theta + \frac{1}{4}\frac{t_c^2}{d^2}\cos^2\theta\right) + \frac{R}{h_c}\left[\frac{\theta}{2} - \frac{R^2}{h_c^2}\sin\theta(1-\cos\theta) - \frac{R}{h_c}\left(2 - 3\frac{R}{h_c}\right)(\theta - \sin\theta)\right]\right\} \tag{21}$$

and h_o appearing in equation (19) is the distance between the middle surface of the face sheet and the panel neutral axis η_o given by

$$h_o = \frac{1}{2\bar{A}}\left[A(h_c + t_c + t_s) + \frac{1}{2}t_c(f_1 - f_2)(t_c + t_s)\right] \tag{22}$$

The twisting stiffness D_{xy} appearing in the expressions of a_{mn}^{rs} (eqs. (11) through (16)) may be obtained from reference 4 with slight modification to fit the present problem in the following form:

$$D_{xy} = 2\overline{GJ} \tag{23}$$

where $\overline{GJ}$ is the torsional stiffness given by

$$\overline{GJ} = \left[G_s t_s k_{\overline{GJ}}^2 + \frac{pG_c t_c^2}{A_c}(k_{\overline{GJ}} - k_c)^2\right]h^2 \tag{24}$$

where

$$k_{\overline{GJ}} = \frac{k_c}{1 + \dfrac{A_c G_s t_s}{pG_c t_c}} \tag{25}$$

and

$$k_c = \frac{1}{2}\left[1 - \frac{(f_1 - f_2)h_c}{2ph}\right] \tag{26}$$

$$A_c = \left[l + \frac{1}{2}(f_1 - f_2)\right]t_c = \bar{l}\,t_c \tag{27}$$

The shear stiffnesses D_{Qx} and D_{Qy} appearing in equations (14) and (16) are given by

$$D_{Qx} = \frac{G_c t_c h^2}{pl},\quad D_{Qy} = \bar{S}h\frac{E_c}{1 - \nu_c^2}\left(\frac{t_c}{h_c}\right)^3 \tag{28}$$

where the nondimensional coefficient $\bar{S}$ is defined as

$$\bar{S} = \frac{6\frac{h_c}{p}D_z^F\frac{t_s}{t_c} + \left(\frac{p}{h_c}\right)^2}{12\left\{\frac{h}{h_c}\frac{p}{h_c}D_z^F - 2\left(\frac{p}{h_c}\right)^2 D_z^H + \frac{h_c}{h}\left[6\frac{t_s}{t_c}(D_z^F D_y^H - D_z^{H^2}) + \left(\frac{p}{h_c}\right)^3 D_y^H\right]\right\}} \tag{29}$$

where the nondimensional parameters D_z^F, D_z^H, and D_y^H are defined as

$$\begin{aligned} D_z^F = {} & \frac{2}{3}\left(\frac{d}{h_c}\right)^3 \cos^2\theta + \frac{2}{3}\frac{I_c}{I_f}\left[\frac{1}{8}\left(\frac{p}{h_c}\right)^3 - \left(\frac{b}{h_c}\right)^3\right] \\ & + \frac{R}{h_c}\left[2\left(\frac{b}{h_c}\right)^2\theta - 4\frac{Rb}{h_c^2}(1-\cos\theta) + \left(\frac{R}{h_c}\right)^2(\theta - \sin\theta\cos\theta)\right] \\ & + \frac{I_c}{h_c^2 t_c}\left[2\frac{d}{h_c}\sin^2\theta + \frac{R}{h_c}(\theta - \sin\theta\cos\theta)\right] \end{aligned} \tag{30}$$

$$\begin{aligned} D_z^H = {} & \frac{2}{3}\left(\frac{d}{h_c}\right)^3 \sin\theta\cos\theta + \frac{1}{2}\frac{I_c}{I_f}\left[\frac{1}{4}\left(\frac{p}{h_c}\right)^2 - \left(\frac{b}{h_c}\right)^2\right] \\ & + \frac{R}{h_c}\left\{\left(\frac{b}{h_c}\right)\theta - 2\frac{Rb}{h_c^2}(\theta - \sin\theta) - \frac{R}{h_c}(1-\cos\theta)\left[1 - \frac{R}{h_c}(1-\cos\theta)\right]\right\} \\ & - \frac{I_c}{h_c^2 t_c}\left(2\frac{d}{h_c}\sin\theta\cos\theta + \frac{R}{h_c}\sin^2\theta\right) \end{aligned} \tag{31}$$

$$\begin{aligned} D_y^H = {} & \frac{2}{3}\left(\frac{d}{h_c}\right)^3 \sin^2\theta + \frac{1}{2}\left(\frac{R}{h_c}\theta + \frac{1}{2}\frac{f}{h_c}\frac{I_c}{I_f}\right) \\ & - \left(\frac{R}{h_c}\right)^2\left[\left(2 - 3\frac{R}{h_c}\right)(\theta - \sin\theta) + \frac{R}{h_c}\sin\theta(1-\cos\theta)\right] \\ & + \frac{I_c}{h_c^2 t_c}\left[\frac{f}{h_c}\frac{t_c}{t_f} + 2\frac{d}{h_c}\cos^2\theta + \frac{R}{h_c}(\theta + \sin\theta\cos\theta)\right] \end{aligned} \tag{32}$$

where

$$f = \frac{1}{2}(f_1 + f_2),\ b = \frac{1}{2}\left[p - \frac{1}{2}(f_1 + f_2)\right],\ I_c = \frac{1}{12}t_c^3,\ I_f = \frac{1}{12}t_s^3 \tag{33}$$

The shear buckling equation (6) yields a set of homogeneous equations associated with different values of *m* and *n*. This set of equations may be divided into two groups that are independent of each other: one group in which $m \pm n$ is odd (that is, antisymmetrical buckling), and the other in which $m \pm n$ is even (that

is, symmetrical buckling) (refs. 7 and 9). Those equations may be written for as many half-wave numbers as required for convergence of eigenvalue solutions. For the deflection coefficients A_{mn} to have values other than zero, the determinant of the coefficients of the unknown A_{mn} of the simultaneous homogeneous equations must vanish. The largest eigenvalue $\frac{1}{k_{xy}}$ thus obtained will give the lowest value of k_{xy}.

Representative 12×12 determinants in terms of the coefficients of homogeneous simultaneous equations written out from equation (6) for which $m \pm n$ is even and odd are given in the following (refs. 10 and 11):

For $m \pm n$ = even (symmetrical buckling):

$m, n \backslash^{i,j}$	A_{11}	A_{13}	A_{22}	A_{31}	A_{15}	A_{24}	A_{33}	A_{42}	A_{51}	A_{35}	A_{44}	A_{53}
m=1, n=1	$\frac{M_{11}}{k_{xy}}$	0	$\frac{4}{9}$	0	0	$\frac{8}{45}$	0	$\frac{8}{45}$	0	0	$\frac{16}{225}$	0
m=1, n=3		$\frac{M_{13}}{k_{xy}}$	$-\frac{4}{5}$	0	0	$\frac{8}{7}$	0	$-\frac{8}{25}$	0	0	$\frac{16}{35}$	0
m=2, n=2			$\frac{M_{22}}{k_{xy}}$	$-\frac{4}{5}$	$-\frac{20}{63}$	0	$\frac{36}{25}$	0	$-\frac{20}{63}$	$\frac{4}{7}$	0	$\frac{4}{7}$
m=3, n=1				$\frac{M_{31}}{k_{xy}}$	0	$-\frac{8}{25}$	0	$\frac{8}{7}$	0	0	$\frac{16}{35}$	0
m=1, n=5					$\frac{M_{15}}{k_{xy}}$	$-\frac{40}{27}$	0	$-\frac{8}{63}$	0	0	$-\frac{16}{27}$	0
m=2, n=4						$\frac{M_{24}}{k_{xy}}$	$-\frac{72}{35}$	0	$-\frac{8}{63}$	$\frac{8}{3}$	0	$-\frac{120}{147}$
m=3, n=3			Symmetry				$\frac{M_{33}}{k_{xy}}$	$-\frac{72}{35}$	0	0	$\frac{144}{49}$	0
m=4, n=2								$\frac{M_{42}}{k_{xy}}$	$-\frac{40}{27}$	$-\frac{120}{147}$	0	$\frac{8}{3}$
m=5, n=1									$\frac{M_{51}}{k_{xy}}$	0	$-\frac{16}{27}$	0
m=3, n=5										$\frac{M_{35}}{k_{xy}}$	$-\frac{80}{21}$	0
m=4, n=4											$\frac{M_{44}}{k_{xy}}$	$-\frac{80}{21}$
m=5, n=3												$\frac{M_{53}}{k_{xy}}$

= 0 (34)

where the nonzero off-diagonal terms satisfy the conditions $m \neq i$, n ≠ j, $m \pm i$ = odd, and $n \pm j$ = odd.

For $m \pm n$ = odd (antisymmetrical buckling):

$m, n \backslash^{i,j}$	A_{12}	A_{21}	A_{14}	A_{23}	A_{32}	A_{41}	A_{16}	A_{25}	A_{34}	A_{43}	A_{52}	A_{61}
m=1, n=2	$\frac{M_{12}}{k_{xy}}$	$-\frac{4}{9}$	0	$\frac{4}{5}$	0	$-\frac{8}{45}$	0	$\frac{20}{63}$	0	$\frac{8}{25}$	0	$-\frac{4}{35}$
m=2, n=1		$\frac{M_{21}}{k_{xy}}$	$-\frac{8}{45}$	0	$\frac{4}{5}$	0	$-\frac{4}{35}$	0	$\frac{8}{25}$	0	$\frac{20}{63}$	0
m=1, n=4			$\frac{M_{14}}{k_{xy}}$	$-\frac{8}{7}$	0	$-\frac{16}{225}$	0	$\frac{40}{27}$	0	$-\frac{16}{35}$	0	$-\frac{8}{175}$
m=2, n=3				$\frac{M_{23}}{k_{xy}}$	$-\frac{36}{25}$	0	$-\frac{4}{9}$	0	$\frac{72}{35}$	0	$-\frac{4}{7}$	0
m=3, n=2					$\frac{M_{32}}{k_{xy}}$	$-\frac{8}{7}$	0	$-\frac{4}{7}$	0	$\frac{72}{35}$	0	$-\frac{4}{9}$
m=4, n=1						$\frac{M_{41}}{k_{xy}}$	$-\frac{8}{175}$	0	$-\frac{16}{35}$	0	$\frac{40}{27}$	0
m=1, n=6			Symmetry				$\frac{M_{16}}{k_{xy}}$	$-\frac{20}{11}$	0	$-\frac{8}{45}$	0	$-\frac{36}{1225}$
m=2, n=5								$\frac{M_{25}}{k_{xy}}$	$-\frac{8}{3}$	0	$-\frac{100}{441}$	0
m=3, n=4									$\frac{M_{34}}{k_{xy}}$	$-\frac{144}{49}$	0	$-\frac{8}{45}$
m=4, n=3										$\frac{M_{43}}{k_{xy}}$	$-\frac{8}{3}$	0
m=5, n=2											$\frac{M_{52}}{k_{xy}}$	$-\frac{20}{11}$
m=6, n=1												$\frac{M_{61}}{k_{xy}}$

$= 0$ (35)

where the nonzero off-diagonal terms satisfy the conditions $m \neq i$, n $\neq j$, $m \pm i =$ odd, and $n \pm j$ = odd.

Notice that the diagonal terms in equations (34) and (35) came from the first term of equation (6), and the series term of equation (6) gives the off-diagonal terms of the matrices. The 12×12 determinant was found to give sufficiently accurate eigenvalue solutions.

NUMERICAL RESULTS

The titanium hat-stiffened panel has the following material properties and geometries:

$E_s = E_c = 6.2 \times 10^6$ lb/in^2
$G_s = G_c = 6.2 \times 10^6$ lb/in^2
$\nu_s = \nu_c = 0.31$
$a = 24$ in.
$b_o = 1.77$ in. (width of rectangular flat strip)
$c = 24$ in.
$d = 0.3505$ in.
$f_1 = 1.12$ in.
$f_2 = 0.26$ in.
$h = h_c + \frac{1}{2}(t_c + t_s) = 1.2180$ in.
$h_c = 1.1860$ in.
$p = 1.49$ in.
$R = 0.346$ in.
$t_s = t_c = 0.032$ in.
$\theta = 79.13° = 1.3811$ rad

Local Buckling

For $a = 24$ in. and $b_o = 1.77$ in., equation (2) gives $k_{xy} = 5.37$. The shear buckling stress $(\tau_{xy})_{cr}$ may then be calculated from equation (1) as

$$(\tau_{xy})_{cr} = 25,553 \text{ lb/in}^2 \tag{36}$$

From equations (4) and (5) the ratio of q_1/q_c has the value

$$\frac{q_1}{q_c} = 3.4727 \tag{37}$$

Thus, from equation (3), the panel shear buckling load $(N_{xy})_{cr}$ may be calculated as

$$(N_{xy})_{cr} = q_1\left(1 + \frac{q_c}{q_1}\right) \tag{38}$$

$$= (\tau_{xy})_{cr} t_s \left(1 + \frac{1}{3.4727}\right) \tag{39}$$

$$= 1,054 \text{ lb/in} \tag{40}$$

which gives the shear buckling load of $Q_{cr} = 25,296$ lb.

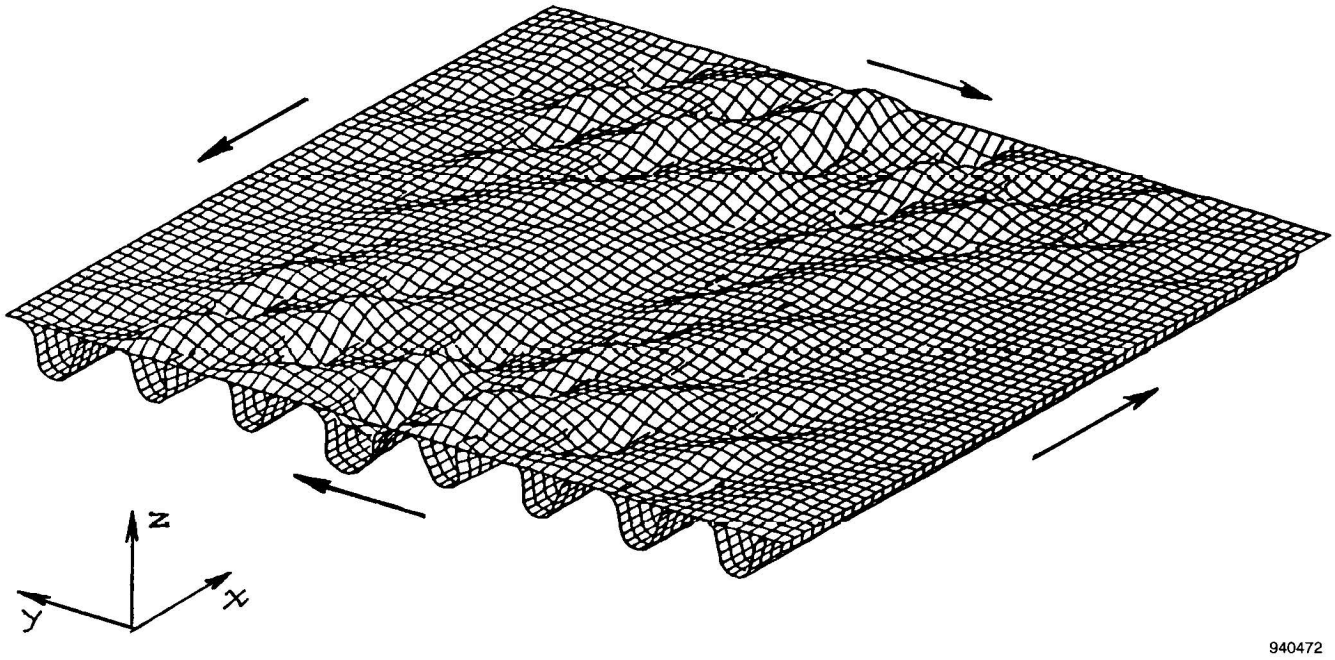

Figure 6. Buckling shape of hat-stiffened panel under shear loading (finite element analysis by W. Percy, Mc-Donnell-Douglas; full-panel model).

This local shear buckling load prediction is slightly higher than the value $(N_{xy})_{cr}$ = 900 lb/in calculated from finite element buckling analysis carried out by W. Percy of McDonnell-Douglas.* Figure 6 shows the shear buckling shape of the hat-stiffened panel based on Percy's full-panel finite element model. Clearly, the panel is under local buckling rather than general instability. The local buckling analysis predicts a slightly higher value of $(N_{xy})_{cr}$ because the four edges of the rectangular plate strip analyzed were assumed to be simply supported. In reality, those four edges are elastically supported.

Global Buckling

To find the order of the determinant (review eqs. (34) and (35)) for converged eigenvalue solutions, several different orders of the determinants were used for the calculations of k_{xy}. The eigenvalues were found to have sufficiently converged beyond order 10. In the actual calculations of k_{xy}, the orders of the determinants were taken to be 12, which were shown in equations (34) and (35). The eigenvalue solutions thus obtained give the following lowest values of k_{xy}:

$$m \pm n = \text{even}: \quad k_{xy} = 1.89 \tag{41}$$

$$m \pm n = \text{odd}: \quad k_{xy} = 1.93 \tag{42}$$

Thus, the square panel will buckle symmetrically. Using k_{xy} = 1.89, the panel shear buckling load $(N_{xy})_{cr}$ may be calculated from equation (10) as

*Personal communication with author.

$$(N_{xy})_{cr} = 4,296 \text{ lb/in} \tag{43}$$

which gives the shear buckling load of $Q_{cr} = 103,107$ lb; this is about four times higher than the local shear buckling load of $Q_{cr} = 25,296$ lb. Thus, the panel is unlikely to fail under global buckling.

Summary of Data

The results of the shear buckling analysis of the hat-stiffened panel are summarized in the following table.

Comparison of shear buckling loads.

Case	$(\tau_{xy})_{cr}$, lb/in	Q_{cr}, lb
Local buckling	1,054	25,296
Global buckling	4,296	103,107
W. Percy's finite element (footnote, p. 15)	900	21,600

CONCLUSION

The shear buckling behavior of a hat-stiffened panel was analyzed in light of local buckling and global buckling. The predicted local buckling loads were slightly higher than those predicted using finite element buckling analysis. The global buckling theory predicted a buckling load about four times higher than was predicted from local buckling theory. Therefore, the hat-stiffened panel will buckle locally instead of globally.

REFERENCES

1. Ko, William L. and Raymond H. Jackson, Compressive Buckling Analysis of Hat-Stiffened Panel, NASA TM-4310, Aug. 1991.
2. Timoshenko, Stephen P. and James M. Gere, *Theory of Elastic Stability*, McGraw-Hill Book Co., New York, 1961.
3. Ko, W. L., "Elastic Stability of Superplastically Formed/Diffusion Bonded Orthogonally Corrugated Core Sandwich Plates," AIAA 80-0683, presented at the AIAA/ASME/ASCE/AHS/AHC 21st Structures, Structural Dynamics, and Materials Conference, Seattle, WA, May 12–14, 1980.
4. Libove, Charles and Ralph E. Hubka, *Elastic Constants for Corrugated-Core Sandwich Plates*, NACA TN-2289, 1951.
5. Libove, C. and S. B. Batdorf, *A General Small-Deflection Theory for Flat Sandwich Plates*, NACA TN-1526, 1948.
6. Bert, Charles W. and K. N. Cho, "Uniaxial Compressive and Shear Buckling in Orthotropic Sandwich Plates by Improved Theory," AIAA 86-0977, presented at the AIAA/ASME/ASCE/AHC 27th Structures, Structural Dynamics, and Materials Conference, San Antonio, TX, May 19–21, 1986.
7. Ko, William L. and Raymond H. Jackson, *Combined Compressive and Shear Buckling Analysis of Hypersonic Aircraft Structural Sandwich Panels*, NASA TM-4290. Also AIAA 92-2487-CP, presented

at the AIAA/ASME/ASCE/AHS/ASC 33rd Structures, Structural Dynamics, and Materials Conference, Dallas, TX, Apr. 13–15, 1992.

8. Ko, William L. and Raymond H. Jackson, *Combined Load Buckling Behavior of Metal-Matrix Composite Sandwich Panels Under Different Thermal Environments,* NASA TM-4321, Sept. 1991.
9. Ko, William L. and Raymond H. Jackson, *Compressive and Shear Buckling Analysis of Metal-Matrix Composite Sandwich Panels Under Different Thermal Environments*, NASA TM-4492, June 1993. Originally prepared for the 7th International Conference on Composite Structures, University of Paisley, Paisley, Scotland, July 1993.
10. Stein, Manuel and John Neff, *Buckling Stresses of Simply Supported Rectangular Flat Plates in Shear*, NACA TN-1222, 1947.
11. Batdorf, S. B. and Manuel Stein, *Critical Combinations of Shear and Direct Stress for Simply Supported Rectangular Flat Plates*, NACA TN-1223, 1947.

REPORT DOCUMENTATION PAGE

Form Approved
OMB No. 0704-0188

1. AGENCY USE ONLY (Leave blank)	2. REPORT DATE	3. REPORT TYPE AND DATES COVERED
	November 1994	Technical Memorandum

4. TITLE AND SUBTITLE

Shear Buckling Analysis of a Hat-Stiffened Panel

5. FUNDING NUMBERS

WU 505-63-40

6. AUTHOR(S)

William L. Ko and Raymond H. Jackson

7. PERFORMING ORGANIZATION NAME(S) AND ADDRESS(ES)

NASA Dryden Flight Research Center
P.O. Box 273
Edwards, CA 93523-0273

8. PERFORMING ORGANIZATION REPORT NUMBER

H-2019

9. SPONSORING/MONITORING AGENCY NAME(S) AND ADDRESS(ES)

National Aeronautics and Space Administration
Washington, DC 20546-0001

10. SPONSORING/MONITORING AGENCY REPORT NUMBER

NASA TM-4644

11. SUPPLEMENTARY NOTES

12a. DISTRIBUTION/AVAILABILITY STATEMENT

Unclassified—Unlimited
Subject Category 39

12b. DISTRIBUTION CODE

13. ABSTRACT (Maximum 200 words)

A buckling analysis was performed on a hat-stiffened panel subjected to shear loading. Both local buckling and global buckling were analyzed. The global shear buckling load was found to be several times higher than the local shear buckling load. The classical shear buckling theory for a flat plate was found to be useful in predicting the local shear buckling load of the hat-stiffened panel, and the predicted local shear buckling loads thus obtained compare favorably with the results of finite element analysis.

14. SUBJECT TERMS

Hat-stiffened panel; Global buckling; Local buckling; Minimum energy method; Shear buckling

15. NUMBER OF PAGES

20

16. PRICE CODE

A03

17. SECURITY CLASSIFICATION OF REPORT	18. SECURITY CLASSIFICATION OF THIS PAGE	19. SECURITY CLASSIFICATION OF ABSTRACT	20. LIMITATION OF ABSTRACT
Unclassified	Unclassified	Unclassified	Unlimited

NSN 7540-01-280-5500

Available from the NASA Center for AeroSpace Information, 800 Elkridge Landing Road, Linthicum Heights, MD 21090; (301)621-0390

Standard Form 298 (Rev. 2-89)
Prescribed by ANSI Std. Z39-18
298-102